Supporting Information

Regenerable sorbent with high capacity for elemental mercury removal and recycling from the simulated flue gas at low temperature

Zan Qu, Jiang-Kun Xie, Hao-Miao Xu, Wan-Miao Chen, and Nai-Qiang Yan*

School of Environmental Science and Engineering, Shanghai Jiao Tong University,

800 Dongchuan Road, Shanghai 200240, China

1. NH_3-TPD curve on $Ce_{0.5}Mn_{0.5}O_y$

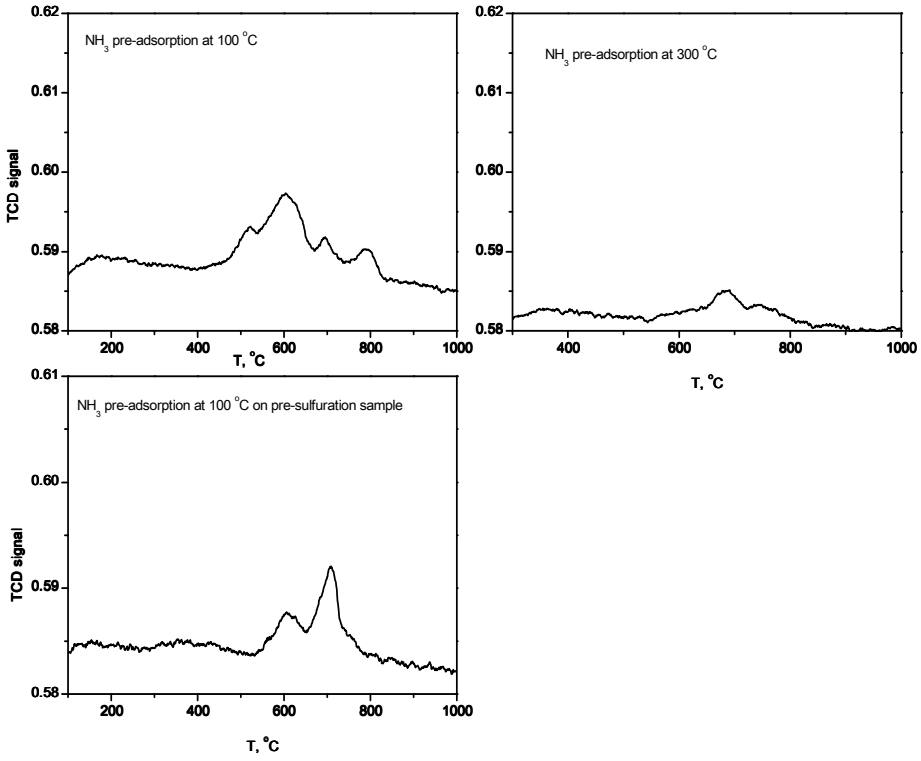

Figure S1. NH_3-TPD curves of $Ce_{0.5}Mn_{0.5}O_y$

* Corresponding author, E-mail address: nqyan@sjtu.edu.cn

(a) adsorbing NH_3 at 100 ^oC,

(b) adsorbing NH_3 at 300 ^oC,

(c) (a) pretreated in 500 ppm SO_2 for 3 h

In order to investigate different adsorption performance of $Ce_{0.5}Mn_{0.5}O_y$ at low and high temperature, NH_3 was pre-adsorbed at 100 and 300 ^oC, after removing the physically adsorbed NH_3 by He purge, temperature-programmed desorption curves were recorded to test its NH_3 adsorption ability. As shown in Figure S1, if NH_3 was pre-adsorbed on the sorbent at 100 ^oC, at least 4 desorption peaks emerged at 500 to 800 ^oC, comparatively, if NH_3 was pre-adsorbed at 300 ^oC, most of the desorption peaks disappeared, the remaining peaks were very weak. It illustrated that NH_3 could easily adsorb on the acidic sites at low temperature, however, most of the acidic sites would lose their activity at high temperature. Furthermore, if the sorbent was pretreated in SO_2 for 3 h, the amount of desorbed NH_3 decreased to some extent compared with non-pretreated sample but the amount of adsorbed NH_3 was still substantial. It's worth noting that some desorption peaks disappeared and relative strength of peaks at 600 ^oC and 700 ^oC changed. It was speculated that SO_2 could competitively adsorb on partial acidic sites and inhibit the adsorption capability of the sorbent. This result was consistent with the mercury adsorption experiment.

2. Ion chromatogram analysis

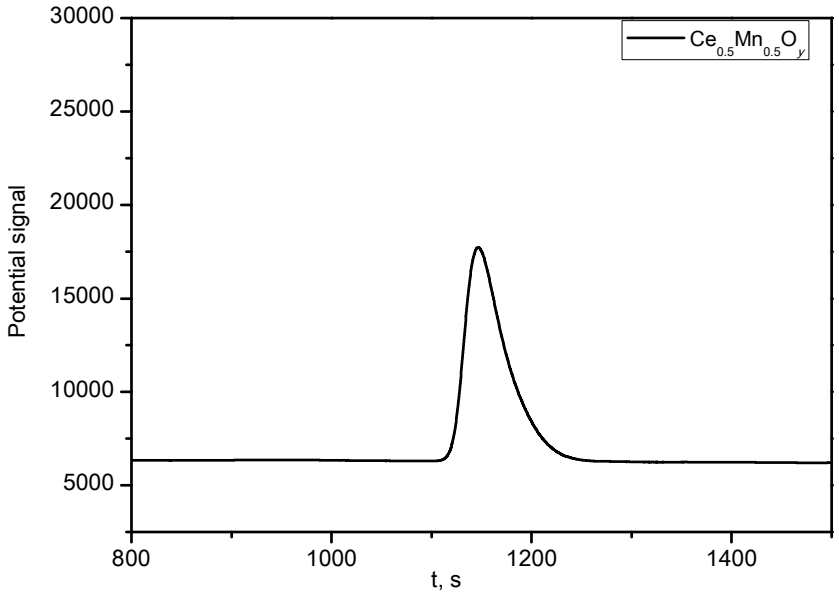

Figure S2. Ion chromatogram for washing solution of $Ce_{0.5}Mn_{0.5}O_y$ after adsorption (with 500 ppm of SO_2)-desorption of mercury

The sorbent after adsorption (with 500 ppm of SO_2)-desorption was immersed into distilled water for 30 min and the supernate was collected and analyzed by ion chromatograph. The result was shown in Figure S2. It was found that the peak emerged at 1100-1200 s was consistent with the peak of sulfate ion. It means that the sulfate salt was formed on sorbent surface after adsorption of mercury under 500 ppm of SO_2 atmosphere. This could explain why SO_2 could to some extent inhibit mercury adsorption.

3. Mercury desorption from $Ce_{0.5}Mn_{0.5}O_y$

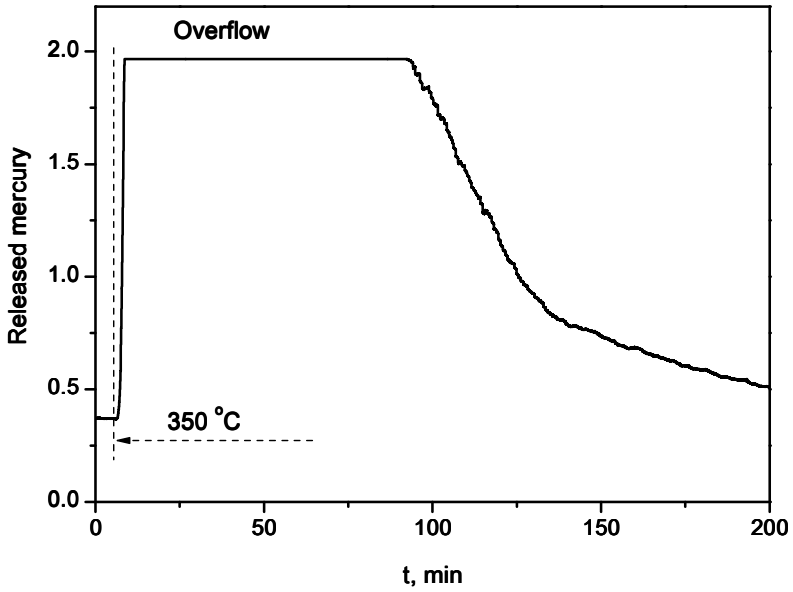

Figure S3. Desorption curve of Hg from $Ce_{0.5}Mn_{0.5}O_y$ at 350 ^oC under N_2 purge

Figure S3 was the mercury desorption curve from spent $Ce_{0.5}Mn_{0.5}O_y$ at 350 ^oC under purge of nitrogen, adsorbed mercury desorbed quickly in the form of elemental mercury. The concentration of desorbed mercury was very high and overflowed the detecting limit of the detector (the released mercury concentration measured by dilution method was higher than 1.2 $mg{\cdot}m^3$).

4. Impact of gas components over $Ce_{0.5}Mn_{0.5}O_y$

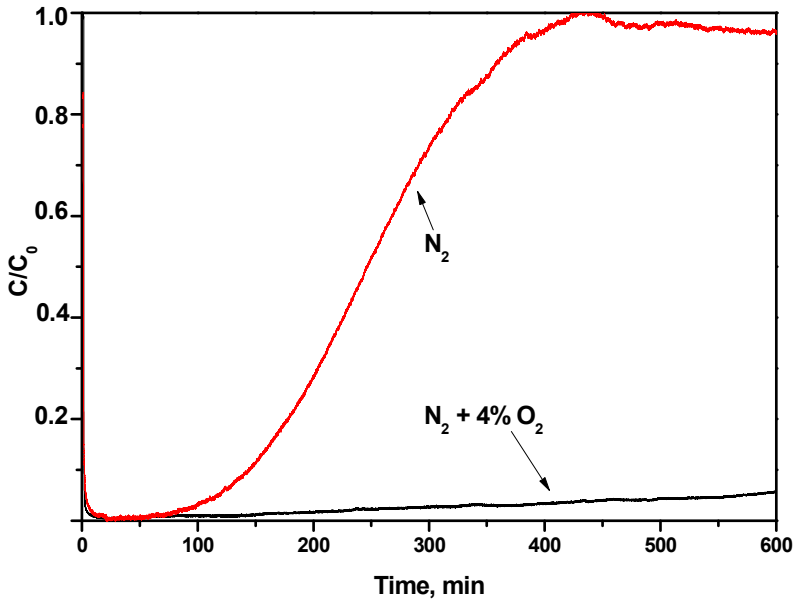

Figure S4. Mercury removal under pure N_2 and N_2 + 4% O_2.

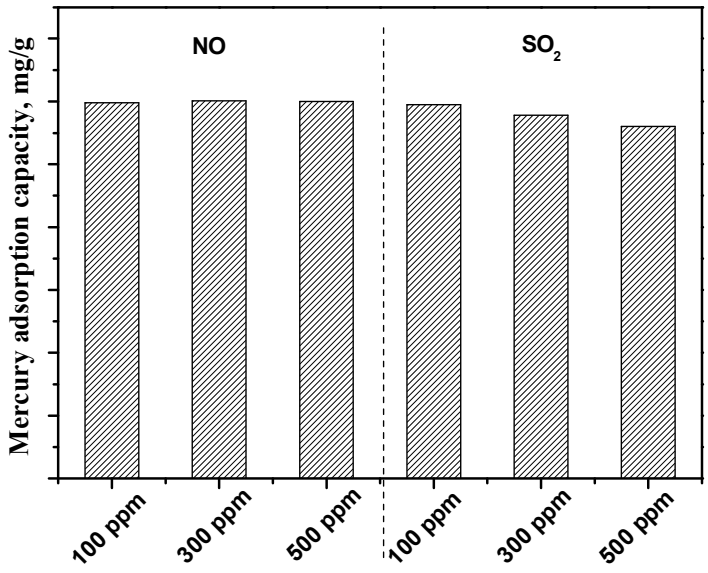

Figure S5. Mercury adsorption capacities at different concentrations of NO and SO_2.

Reaction conditions: 4% O_2, 100 ^{o}C.

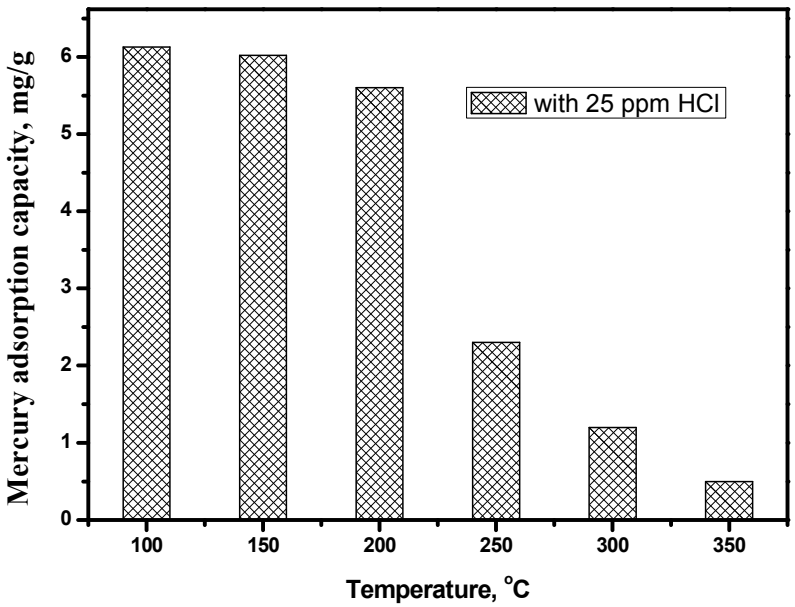

Figure S6. Impact of HCl on adsorption capacity of $Ce_{0.5}Mn_{0.5}O_y$ at different test temperature.

5. Mercury desorption activation energy calculation

Assumed that the desorption process follows first-order kinetics[1-3]:

$$\frac{r_d}{N_s} = -\frac{\mathrm{d}\theta}{\mathrm{dt}} = k_d\theta \qquad \text{(S1)}$$

Where r_d denotes desorption rate of mercury from sorbent (mol·min^{-1}), Ns denotes the maximum mercury concentration on unit surface of sorbent (mol·cm^{-2}), θ denotes the transient coverage of mercury and t is the time (min), kd is the desorption rate coefficient and defined as follows:

$$k_d = A\exp(-\frac{E_d}{\mathrm{RT}}) \qquad \text{(S2)}$$

Where E_d is the desorption activation energy (kJ·mol^{-1}), R is gas constant, T is temperature, A is pre-exponential factor. Combining equation S1 and equation S2, equation S3 could be obtained.

$$\frac{r_d}{N_s} = -\frac{\mathrm{d}\theta}{\mathrm{dt}} = A\,\theta\exp(-\frac{E_d}{\mathrm{RT}}) \qquad \text{(S3)}$$

Assumed that the initial temperature of TPD experiment was T_0 (K), and the heating rate was β (K·min^{-1}), so reaction temperature varies with time following equation S4:

$$\mathrm{T} = T_0 + \beta\mathrm{t} \qquad \text{(S4)}$$

With the elevation of temperature, mercury on sorbent surface desorbs gradually. Assumed that the desorption rate reaches the maximum value at a certain temperature T_p (K), then $\frac{dr_d}{\mathrm{dt}} = 0$, and time derivative of equation S3 can be expressed by equation S5:

$$\frac{1}{\mathrm{N_s}}\frac{\mathrm{dr_d}}{\mathrm{dt}} = \mathrm{A}\,\frac{\mathrm{d}\theta}{\mathrm{dt}}\exp\left(-\frac{\mathrm{E_d}}{\mathrm{RT_p}}\right) + \mathrm{A}\,\theta\,\frac{\mathrm{E_d}}{\mathrm{R}}\frac{1}{\mathrm{T_p^2}}\exp\left(-\frac{\mathrm{E_d}}{\mathrm{RT_p}}\right)\frac{\mathrm{dT}}{\mathrm{dt}} = 0 \qquad \text{(S5)}$$

Combining with equation S4, equation S5 could be written as equation S6:

$$\ln\frac{\beta}{\mathrm{RT}_p^2} = -\frac{E_d}{\mathrm{RT}_p} - \ln\frac{E_d}{A} \qquad \text{(S6)}$$

Equation S6 can be further revised as equation S7:

$$2\ln\mathrm{T_p} - \ln\beta = \frac{\mathrm{E_d}}{\mathrm{RT_p}} + \ln\frac{\mathrm{E_d}}{\mathrm{AR}} \qquad \text{(S7)}$$

Based on Hg-TPD curves under different heating rate, making plot of $(2\ln\mathrm{T_p} - \ln\beta)$

against $\frac{1}{T_p}$, a linear relation can be generated. According to slope and intercept, E_d and A could be calculated and the result was listed in Table S1.

Table S1 Calculation of mercury desorption activation energy from $Ce_{0.5}Mn_{0.5}O_y$ surface

Peak number	Desorption temperature under different heating rate, °C			Desorption activation energy, kJ·mol^{-1}
	2 °C·min^{-1}	5 °C·min^{-1}	10 °C·min^{-1}	
1st peak	255.8	262.5	291.0	89.4
2nd peak	331.8	347.0	368.0	131.3

Table S2 Mercury capacity of sorbents at 100 to 300 °C (Corresponding to Figure 6, data have been rounded, mg·g^{-1})

Sorbents	CeO_2	$Ce_{0.75}Mn_{0.25}O_y$	$Ce_{0.5}Mn_{0.5}O_y$	$Ce_{0.25}Mn_{0.75}O_y$	MnO_y
100 °C	0.05	5.87	6.02	5.94	3.06
200 °C	0.04	3.76	5.00	4.68	1.53
300 °C	0.03	0.22	0.42	0.41	0.05

Table S3 Mercury capacity of $Ce_{0.5}Mn_{0.5}O_y$ under different simulated flue gas condition (Corresponding to Figure 7, all data have been rounded, mg·g^{-1})

$Ce_{0.5}Mn_{0.5}O_y$	N_2+O_2	N_2+O_2+ 500 ppm NO	N_2+O_2+ 500 ppm SO_2	N_2+O_2+ 500 ppmSO_2+2% H_2O
100 °C	6.02	6	5.61	3.95
150 °C	5.86	5.8	5.46	3.66
200 °C	5.00	4.9	4.66	3.43
250 °C	0.93	1.02	0.86	0.8
300 °C	0.42	0.43	0.39	0.36
350 °C	0.04	0.03	0.04	0.06

Reference

[1] H.X. Xi, Z. Li, H.B. Zhang, X. Li, X.J. Hu, Estimation of Activation Energy for Desorption of Low-Volatility Dioxins on Zeolites by TPD Technique, Sep. Purif. Technol. 31 (2003) 41-45.

[2] Z. Li, H.J. Wang, H.X. Xi, Q.B. Xia, J.L. Han, L.A. Lu, Estimation of Activation Energy of Desorption of n-Hexanol from Activated Carbons by the TPD Technique, Adsorpt. Sci. Technol. 21 (2003) 125-133.

[3] R.T. Yang, R.Q. Long, J. Padin, A. Takahashi, T. Takahashi, Adsorbents for Dioxins: A New Technique for Sorbent Screening for Low-Volatile Organics, Ind. Eng. Chem. Res. 38 (1999) 2726-2731.